NANO LETTERS

pubs.acs.org/NanoLett

Letter

Bright and Dark Exciton Coherent Coupling and Hybridization Enabled by External Magnetic Fields

Varun Mapara, Arup Barua, Volodymyr Turkowski, M. Tuan Trinh, Christopher Stevens, Hengzhou Liu, Florence A. Nugera, Nalaka Kapuruge, Humberto Rodriguez Gutierrez, Fang Liu, Xiaoyang Zhu, Dmitry Semenov, Stephen A. McGill, Nihar Pradhan, David J. Hilton, and Denis Karaiskaj*

Cite This: *Nano Lett.* 2022, 22, 1680−1687

Read Online

ACCESS | Metrics & More | Article Recommendations | Supporting Information

ABSTRACT: Magnetic field- and polarization-dependent measurements on bright and dark excitons in monolayer WSe_2 combined with time-dependent density functional theory calculations reveal intriguing phenomena. Magnetic fields up to 25 T parallel to the WSe_2 plane lead to a partial brightening of the energetically lower lying exciton, leading to an increase of the dephasing time. Using a broadband femtosecond pulse excitation, the bright and partially allowed excitonic state can be excited simultaneously, resulting in coherent quantum beating between these states. The magnetic fields perpendicular to the WSe_2 plane energetically shift the bright and dark excitons relative to each other, resulting in the hybridization of the states at the K and K′ valleys. Our experimental results are well captured by time-dependent density functional theory calculations. These observations show that magnetic fields can be used to control the coherent dephasing and coupling of the optical excitations in atomically thin semiconductors.

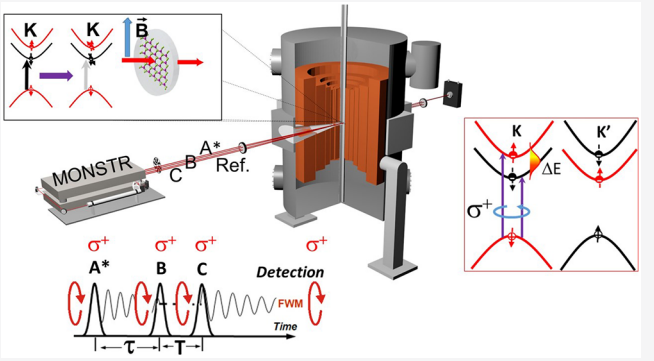

KEYWORDS: *Nonlinear optical spectroscopy, Four-wave mixing spectroscopy, Two-dimensional excitons, Transition metal dichalcogenides, Time-dependent DFT*

INTRODUCTION

Transition metal dichalcogenide (TMD) monolayers exhibit a band structure with spin-valley locking due to their broken inversion symmetry and strong spin−orbit coupling.[1−8] The lack of inversion symmetry gives rise to the spin-valley polarization, whereas the strong spin−orbit interaction results in the splitting of the conduction and valence band extrema, forming spin allowed and forbidden direct excitons. Their lowest energy photoexcitations in different valleys can be excited by circularly polarized light of opposite handedness, leading to circular dichroism..[9−12] The energy splitting of these extrema varies in size. Whereas the valence band splitting is large, in the order of hundreds of millielectronvolts, the conduction band splitting is in the order of few tens of millielectronvolts.[13] The alignment order of dark and bright exciton energy levels depends on the chemical composition of the materials. Experimental and theoretical work has shown that the lowest energy exciton in $MoSe_2$ monolayers is spin-allowed leading to optically bright excitons, whereas in MoS_2, WS_2, and WSe_2 monolayers the lowest state is spin forbidden, forming dark excitons.[14−17] Thus, these monolayer materials have a low photoluminescence quantum efficiency at low temperatures. At a higher temperature, the bright exciton state can be thermally activated from the dark spin forbidden state and hence can emit photons. In WSe_2 monolayer, the photoluminescence is quenched at temperatures below 80 K, implying to an activation energy of ∼30 meV.[18]

Although dark excitons are optically inactive, they play an essential role in the optical properties of these materials, as they provide alternative decay channels via many-body interactions, which affect the lifetime and coherence of bright excitons. Therefore, probing the interaction of dark and bright excitons using coherent optical excitations, is important for both, fundamental understanding and applications of 2D materials.[19] There are several methods to manipulate dark excitons such as via resonant internal transition from bright excitonic states,[20] the application of an external magnetic field,[16,17,21,22] near-field dark exciton-surface plasmon polariton coupling,[23] and Purcell-enhanced dark exciton emission using tip-enhanced photoluminescence[24] via exciton−phonon inter-

Received: December 6, 2021
Revised: January 28, 2022
Published: February 7, 2022

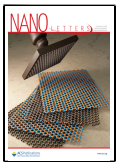

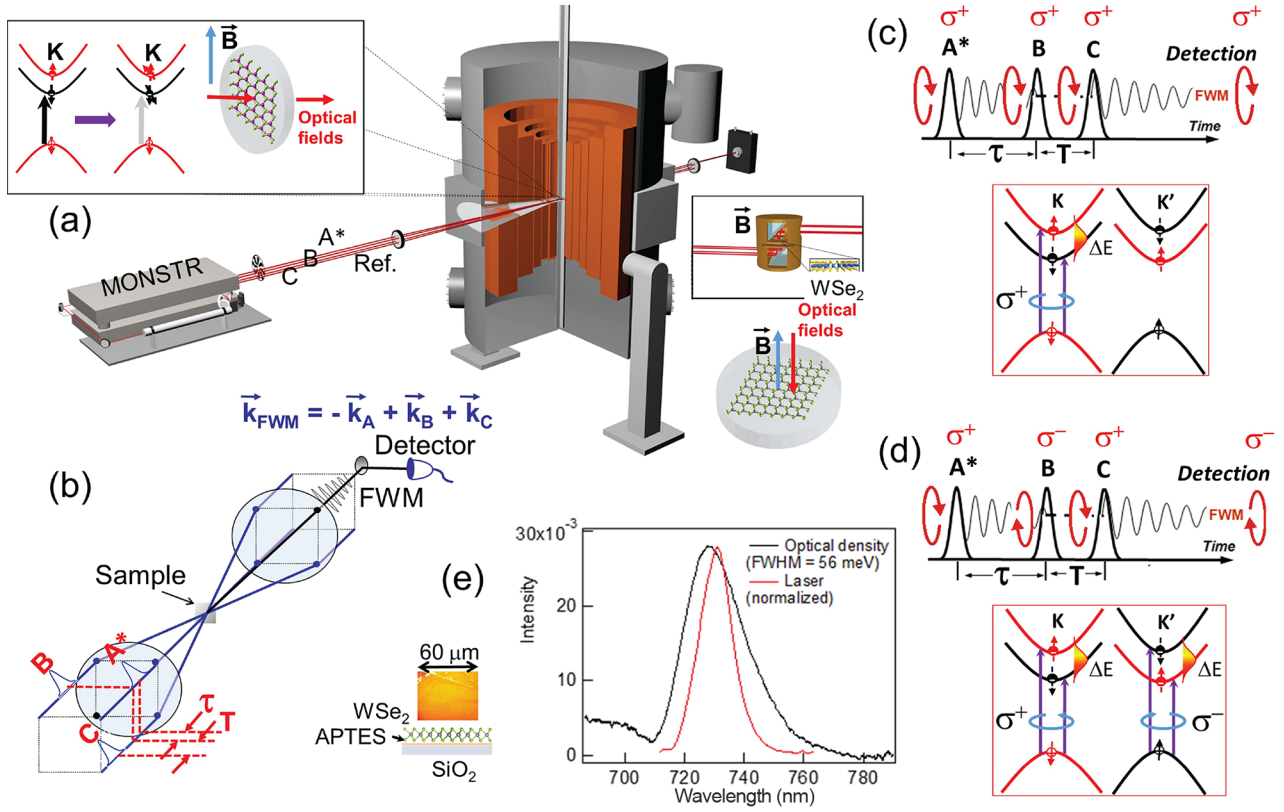

Figure 1. Experimental setup using the resistive 25 T magnet.(a) Experimental setup using the 25 T Split-Helix magnet and the multidimensional optical nonlinear spectrometer (MONSTR). (b) The excitation pulses are arranged in the box-geometry with the pulse A* and B separated by the dephasing τ, and pulses B and C separated by the population time T. The time-integrated FWM signal is detected in the missing corner by the photodiode. The magnetic field is either in parallel or in perpendicular to the sample. The parallel magnetic field cants the spins and brightens the lowest spin forbidden dark state. In the case of the perpendicular field, we used a custom designed sample holder. (c) The cocircular polarization sequence ($\sigma^+\sigma^+\sigma^+\sigma^+$), where all laser pulses are circularly polarized with the same handiness σ^+, including the detection. (d) The cross-circular polarization sequence ($\sigma^+\sigma^-\sigma^+\sigma^-$), where each polarization handiness corresponds to the laser pulses A*, B, C, and detection, respectively. (e) Optical image and sample layout of the large area exfoliated WSe_2 monolayer. The absorption spectrum of the large area WSe_2 monolayer at 7 K. The red curve is the excitation laser spectrum.

action.[25] Recently, the application of a strong external magnetic field perpendicular to the monolayer plane of $MoSe_2$ showed that the coherent nonlinear optical response was dominated by the formation of biexcitons.[26] This demonstrates that magnetic fields can serve as a control to enhance quasiparticle formation and help search for more exotic states of matter.

Furthermore, by applying external magnetic fields, the spin states and valley degeneracy can be manipulated. In the present study we consider both cases, where the magnetic field is applied in-plane (parallel) and out-of-plane (perpendicular) to the monolayer material. The out-of-plane magnetic field application leads to lifting of the valley degeneracy due to the Zeeman effect. Large magnetic fields are required to observe the Zeeman splitting of excitons in monolayer TMDs.[3,11,27] Recent reports indicate that the valley splitting in monolayer WSe_2 can be greatly enhanced due to the interfacial magnetic exchange field from a ferromagnetic substrate.[28] The Zeeman splitting can be observed at perpendicular magnetic fields, whereas for parallel magnetic fields is unimportant. However, parallel fields can tilt the spins, resulting in a mixed spin state, making the spin forbidden transitions partially allowed. This was observed in photoluminescence studies, where photon emission from the dark excitons was enhanced by the application of in-plane magnetic fields, a phenomenon called brightening the dark excitons.[14,21] In such conditions, the photoluminescence intensity ratio between the dark and the bright excitons was found to be quadratically dependent on the applied magnetic field.[14,16,17]

The physical picture becomes more interesting at very short time scales and under coherent excitations. The dephasing time is a fundamental parameter of the exciton quantum dynamics and is sensitive to many-body interactions, serving as a tool for examining them. Furthermore, being atomically thin leads to the reduction of the Coulomb screening, making them an ideal system to study many-body Coulomb interactions. Although the optical and transport properties of monolayer TMDs at high magnetic fields have been intensively studied, the coherent coupling and interactions of dark and bright excitons remains largely unexplored.[3,11,14,16,17,21,22,26,27,29] The reason lays in the difficulty of such measurements due to the small size of exfoliated monolayer TMDs. Diffraction limited optics is extremely challenging to implement in large magnets without the use of optical fibers. Furthermore, detecting the coherence of photoexcitations is very important in the condensed matter physics community. A long coherent spin lifetime is key to the realization of quantum computing, because it allows the time to manipulate the spins and quantum entanglement. In that context, the dark exciton is of great interest for quantum computing applications because of

https://doi.org/10.1021/acs.nanolett.1c04667
Nano Lett. 2022, 22, 1680−1687

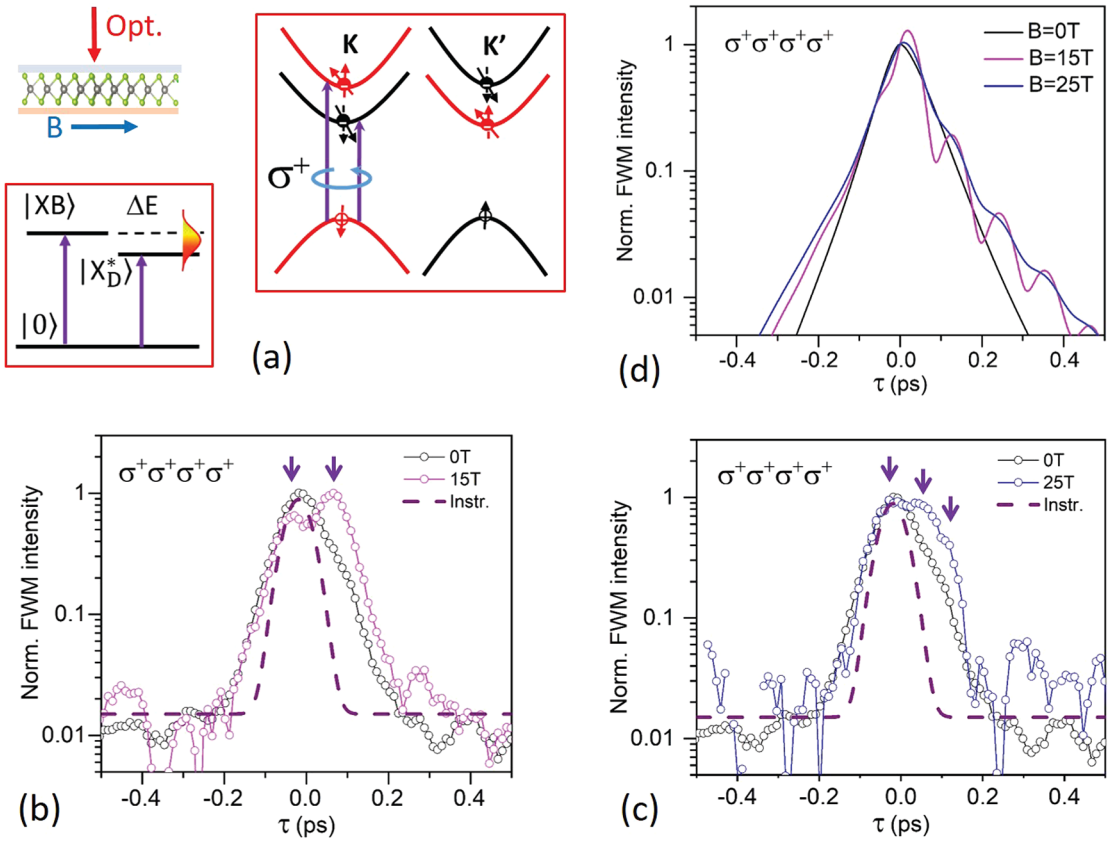

Figure 2. Coherent coupling enabled by an in-plane magnetic field. (a) Schematic of the excitation. The magnetic field parallel to the monolayer WSe_2 brightens the lower spin forbidden lower state. The laser pulse excites both states simultaneously. The cocircular ($\sigma^+\sigma^+\sigma^+\sigma^+$) polarization sequence generates excitons only in one valley. (b,c) Quantum beating under the parallel magnetic field for cocircular polarization configuration. Time-integrated FWM signals under magnetic fields of 15 T (b) and 25 T (c) for a large area exfoliated monolayer WSe_2 at 10 K. The dashed line is the instrumental response. (d) Time-dependent DFT calculations for the parallel field the monolayer WSe_2, showing a quantum beating between dark and bright states for 15 and 25 T. The beating is absent at zero fields.

its long lifetime. However, being spin forbidden makes it difficult to access and manipulate optically. The possible coupling between the dark and bright excitons facilitated by a magnetic field is an intriguing way to optically access the dark states.

Here, we show that it is possible to manipulate the dark and bright exciton through coherent coupling facilitated by a strong magnetic field. External magnetic fields can hybridize the bright and dark excitons in various ways, depending on the relative direction and strength of the field. In-plane magnetic fields lead to an increase of the dephasing time of the bright exciton, by making the dark spin forbidden exciton partially allowed. Most importantly, it allows access to the optically dark exciton and enables coherent coupling with the optically allowed bright exciton.

RESULTS

In-Plane Magnetic Field. We start our discussion with the magnetic field applied parallel to the TMD plane. The effect of the magnetic field is shown schematically in Figure 1a, where the spins are canted by the field and the lowest spin forbidden transition (black arrow) becomes partially allowed or brightened (gray arrow). The three laser pulses A*, B, and C were focused on the sample held at 10 K centered inside the magnet bore and were separated by the time delays τ and T, generating a four wave mixing (FWM) signal in the phase-matching direction $-\mathbf{k}_A + \mathbf{k}_B + \mathbf{k}_C$, illustrated in Figure 1b. Two different circularly polarized sequences were used, ($\sigma^+\sigma^+\sigma^+\sigma^+$) and ($\sigma^+\sigma^-\sigma^+\sigma^-$), labeled here as cocircular and cross-circular, respectively and are shown together with their induced excitations in Figure 1c,d. The time delay τ between the A* and B/C pulses measures the coherence or dephasing time. The spectral width of the laser pulse allows for the simultaneous excitation of both the lower spin forbidden and upper spin allowed transition. The band diagram is shown in Figure 2a, where the cocircular ($\sigma^+\sigma^+\sigma^+\sigma^+$) polarization sequence excites and probes only the K valley. We measure the time-integrated FWM at two magnetic fields, 15 and 25 T, and compare the dynamics with the measurement at zero field.

Previous time-integrated FWM studies have indicated that the dephasing time in monolayer TMDs is limited by efficient electron−phonon scattering and short radiative recombination, leading to large homogeneous broadening of the transition.[30−32] However, later measurements on boron nitride encapsulated TMDs have shown lower excitonic line widths, indicating longer radiative decays.[33−35] The time-integrated FWM at 15 T is compared with measurements on the same WSe_2 sample at zero magnetic field in Figure 2b. At zero field, we obtain a dephasing time T_2 of ∼250 fs. This is well in agreement with our previous measurement on exfoliated samples of ∼279 fs[30] and other reports of ∼250 fs for exfoliated and CVD grown WSe_2 monolayer.[32] The measured dephasing time T_2 is related to the homogeneous line width γ by a simple relationship $\gamma = 2\hbar/T_2$ and corresponds to an

https://doi.org/10.1021/acs.nanolett.1c04667
Nano Lett. 2022, 22, 1680−1687

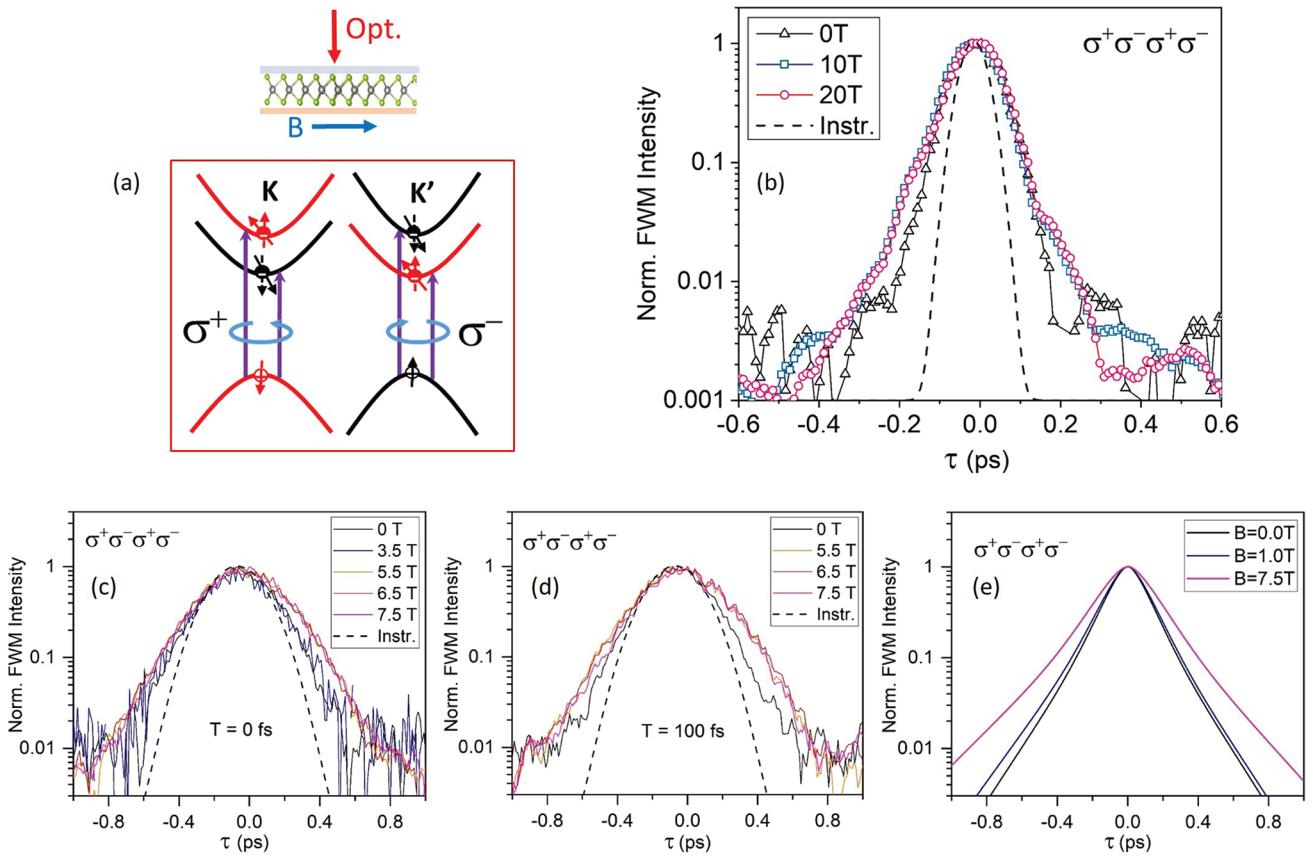

Figure 3. Increased coherence by the dark exciton generated by the in-plane magnetic field. (a) Schematic of the excitation. The magnetic field parallel to the monolayer WSe_2 brightens the lower spin forbidden lower state. In the cross-circular polarization sequence, the first pulse excites and generates an exciton in the K valley, whereas the second pulse generates an exciton in the K′ valley. (b) Time-integrated FWM at 10 and 20 T for large area exfoliated monolayer WSe_2 at 10 K. The dashed line corresponds to the instrumental response. (c,d) The time integrated FWM as a function of the dephasing time τ at the population times T = 0 fs (c) and T = 100 fs (d), respectively. The dashed line corresponds to the instrumental response. (e) Time-dependent DFT calculations for the parallel field for the monolayer WSe_2 at B = 0 T, B = 1 T, and B = 7.5 T.

intrinsic homogeneous line width of ∼5 meV,[32] which is 1 order of magnitude smaller than the inhomogeneous line width. A quickly decaying oscillation is observed at 15 T with a period of ∼100 fs as a function of the delay time τ. Such coherent oscillations in the FWM signal have been observed previously in GaAs quantum wells[36−38] and CdS single crystals[39] and were attributed to the coherent quantum beating between light- and heavy-hole states that were concurrently excited by a broadband femtosecond laser pulse. Recently, the quantum beating between exciton and trion states has been observed in $MoSe_2$ and a few layer ReS_2.[40,41]

The excitation laser pulses are spectrally broad and simultaneously excite both conduction band states as shown in Figure 2a. The energy separation corresponding to a beating period of ∼100 fs is $\Delta E = h/\Delta\tau$ = 38 meV, consistent with the energy separation between the spin-split conduction bands, which is predicted to be ∼38 meV. These oscillations with the same period are observed at 25 T, shown in Figure 2c. The FWM signal oscillation is less pronounced than at 15 T due to the larger hybridization of the bright and dark excitons at higher magnetic fields. Finally, we perform time-dependent density functional theory (TD-DFT) calculations to further elucidate the nature of the observed oscillations. Both biexciton and non-Markovian memory effects were included in the calculations.[26] The theoretical curves are shown in Figure 2d, for 0, 15, and 25 T. The theoretical calculations confirm the observed oscillation as originating from the coherent coupling of the upper bright state and the lower weakly allowed "brightened" state. The less pronounced oscillations at 25 T are also well reproduced and attributed to the stronger hybridization of the bright and dark excitons.

We rule out polarization interference[42] or population oscillations involving coherent phonons,[43] or biexcitons,[44] since no oscillations were observed at zero-field or low fields and no beating was observed for cross-circular polarization. In the latter case, the simultaneous excitation of the dark and bright states needs to take place in the same valley and thus share the same ground state, to observe quantum beating. The coherent beating between neutral and charged excitons has been observed at zero fields because of their accessible energy separation by the spectral width of the laser pulse.[40,45] However, the ability to generate quantum coherent coupling between the bright and the spin forbidden state using external magnetic fields opens new avenues to accessing the much longer-lived dark exciton state and enables the applications in quantum computation and quantum entanglement.

We explore the same in-plane orientation of the magnetic field further by using the cross-circular ($\sigma^+\sigma^-\sigma^+\sigma^-$) polarization sequence. In the cross-circular polarization sequence, the first pulse excites and generates an exciton in the K valley, whereas the second pulse excites the K′ valley. Since the two excitons do not share the same ground state, no quantum beating is

https://doi.org/10.1021/acs.nanolett.1c04667
Nano Lett. 2022, 22, 1680−1687

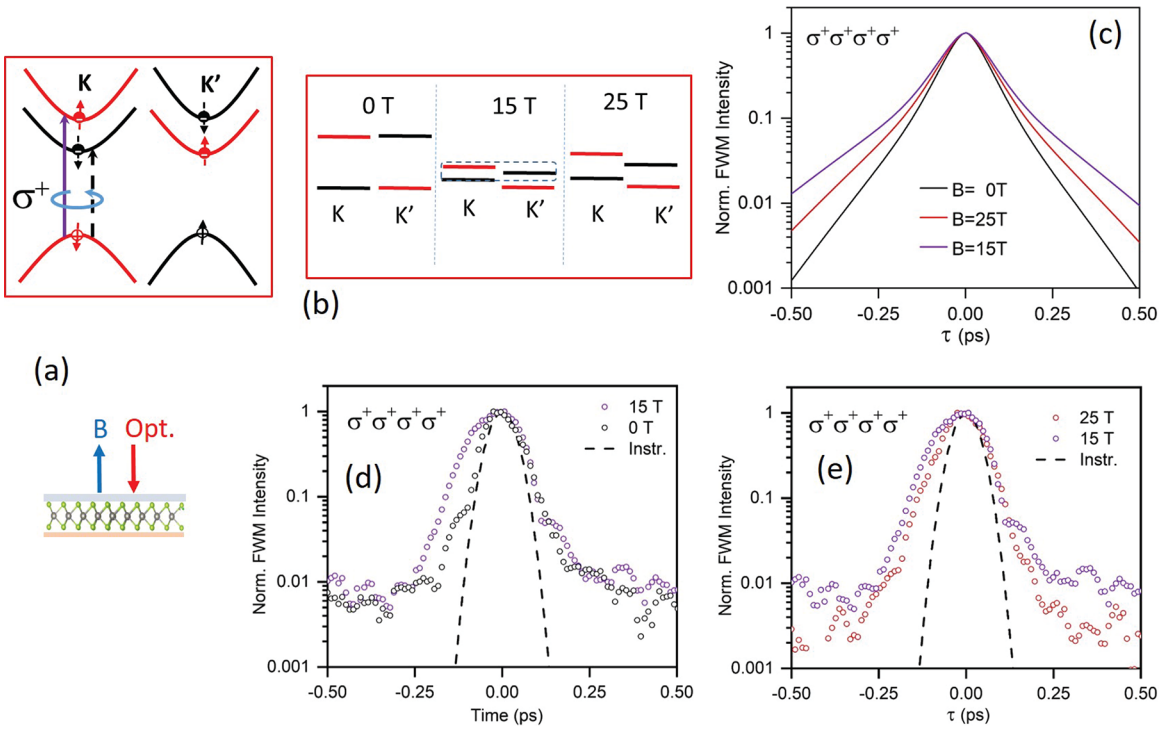

Figure 4. Increased coherence from the hybridization of the bright-dark states facilitated by the out-of-plane magnetic field. (a) Schematic of the excitation. The cocircular ($\sigma^+\sigma^+\sigma^+\sigma^+$) polarization sequence generates excitons only in one valley. (b) Zeeman shift of the bright and dark exciton levels at 15 and 25 T as compared to zero field. The stronger hybridization of the bright and dark excitons at 15 T leads to the strongest increase in dephasing time. (c) Time-dependent DFT calculated FWM signal in monolayer WSe_2 at perpendicular fields using cocircularly polarized excitations. The calculations are shown for zero fields and for 15 and 25 T. The time prolong is more dominant for 15 T than that of 25 T. (d) Experimental time-integrated FWM for cocircular polarizations comparing the dephasing at 0 and 15 T. (e) Comparison of the experimental time-integrated FWM between 15 and 25 T. The measurements were conducted on WSe_2 monolayers at 10 K.

expected in this case. However, biexciton formation can lead to quantum beating, where the period of the oscillations corresponds to the energy separation between the exciton and biexciton, thus the biexciton binding energy. With cross-circular polarizations, the signal beating due to biexcitons is expected to be enhanced, as observed for $MoSe_2$.[44] Using cross-circular polarizations we observe an increase in the dephasing time $T_2 \sim 280$ fs due to the brightening of the lower state, but we do not observe quantum beating oscillations. This excludes the role of biexcitons as the possible source of the quantum beating at cocircular polarizations. The increase in the dephasing time T_2 with the in-plane magnetic field can be observed in Figure 3b at 10 and 20 T. In order to explore the low field limit in which a change in the dephasing time is observed, we implement a smaller magnet with a maximum field up to 7.5 T. The time-integrated FWM is shown in Figure 3c,d, for two time delays $T = 0$ fs and $T = 100$ fs, respectively. The increase in the dephasing time T_2 is experimentally observable starting from 5.5 T and above and this behavior is well captured by the theoretical simulations in Figure 3e using TD-DFT.

Out-of-Plane Magnetic Field. After having investigated the quantum beating between dark and bright states due to spin mixing at parallel fields, we continue our discussion with the interactions between the bright and dark excitons when subjected to large magnetic fields perpendicular to the WSe_2 monolayer plane. Under an out-of-plane magnetic field, the cyclotron energy for the magnetic fields used in this study (7.5−25 T) is estimated to be between ∼27 and ∼50 meV. These values are much smaller than the reported exciton binding energy in a monolayer of WSe_2, ∼200−400 meV. Further comparison of the magnetic length at these fields $l_B = \sqrt{\frac{\hbar}{eB}} = \frac{25.6}{\sqrt{B(T)}}$ nm = 5.1−9.34 nm results in values much larger than the zero-field exciton radius (∼1 nm) in monolayer WSe_2. Therefore, Landau levels are not expected to contribute at these perpendicular magnetic fields but can rather be treated as a perturbation by the field. The exciton wave functions and energies can be approximated by their field-independent values and the only magnetic field effect we consider is the Zeeman shift of the energy levels. The Zeeman shift of the conduction and valence bands due to external magnetic fields perpendicular to the monolayer has been measured[3,11,46,47] The total energy shift is the result of the spin ($g_s s_z \mu_B B$), orbital $\left(\frac{m_e}{m^*} n \mu_B B\right)$, and valley ($m_a n \mu_B B$) contributions, where $n = \pm 1$ is the valley index and m_a is a magnetic quantum number, leading to opposite energy shifts of the K and K′ valleys.[22]

Previous studies have shown that both, polarizations and magnetic fields can affect the exciton dephasing in monolayer $MoSe_2$.[26] One way that magnetic fields applied perpendicular to the WSe_2 plane can affect the excitonic dephasing is through the relative Zeeman shift between the dark and bright excitons. We calculate the relative energy shifts of the excitons at the K and K′ valleys at 15 and 25 T using TD-DFT and compare it to zero fields. The relative positions are schematically shown in Figure 4b. The bright and dark exciton states are closer energetically at 15 T and then move further apart at 25 T, thus resulting in a stronger hybridization at 15 T. The theory predicts that this behavior should affect the excitonic

https://doi.org/10.1021/acs.nanolett.1c04667
Nano Lett. 2022, 22, 1680−1687

dephasing decay observed in time-integrated FWM. Because of the hybridization of the dark and bright excitons, the radiative lifetime of the bright excitons increases, leading to a small, but measurable increase of the observed exciton dephasing time. Indeed, the theoretical calculations of the dephasing dynamics are shown in Figure 4c showing the largest T_2 increase for 15 T and a smaller increase for 25 T. This seemingly counterintuitive behavior is explained by the relative energy shift of the excitons shown in Figure 4b. The closer energetically the bright and dark excitons are, the stronger they hybridize. This is captured experimentally in Figure 4d,e, where the time-integrated FWM is compared for 0 and 15 T in Figure 4d and 15 and 25 T in Figure 4e, respectively. The theoretical calculations predict a slower rise and decay dynamics for negative and positive delays in the time-integrated FWM signal, where the negative delay FWM signal is due to two-exciton (four-particle) correlations and can lead to non-Markovian memory effects.[26,48,49] Although the effect is small, the experimental data captures the effect and the trend with increasing magnetic fields. The dephasing time T_2 is longer at 15 T as compared to zero fields but decreases or possibly remains unchanged at 25 T compared to 15T.

CONCLUSIONS

In this article, we demonstrate the importance of bright−dark exciton hybridization in the coherent dynamics of monolayer WSe_2, where the lower state is spin forbidden. The in-plane magnetic field leads to a partial brightening of the dark exciton, and we observe coherent coupling with the bright exciton. Our observation shows that magnetic fields can be used to control the coherent dephasing time and the coupling of the optical excitations in atomically thin semiconductors. The in-plane magnetic fields allow access to the dark excitons leading to the coherent beating between the dark and bright states under a broadband femtosecond pulse. At perpendicular fields, the Zeeman energy shifts lead to the hybridization of the dark and bright excitons, resulting in longer dephasing times. The coherent quantum beating between different spin states plays a crucial role in understanding intriguing coherent phenomena that enable quantum computing applications in atomically thin semiconductors.

ASSOCIATED CONTENT

Supporting Information

The Supporting Information is available free of charge at https://pubs.acs.org/doi/10.1021/acs.nanolett.1c04667.

Additional experimental details, materials, methods, including additional drawing of experimental setup and theoretical formalism used in the time-dependent DFT calculations (PDF)

Accession Codes

All data are available in the main text or the Supporting Information.

AUTHOR INFORMATION

Corresponding Author

Denis Karaiskaj − *Department of Physics, University of South Florida, Tampa, Florida 33620, United States;* orcid.org/0000-0002-3181-7545; Email: karaiskaj@usf.edu

Authors

Varun Mapara − *Department of Physics, University of South Florida, Tampa, Florida 33620, United States*

Arup Barua − *Department of Physics, University of South Florida, Tampa, Florida 33620, United States*

Volodymyr Turkowski − *Department of Physics, University of Central Florida, Orlando, Florida 32816, United States*

M. Tuan Trinh − *Department of Physics, University of South Florida, Tampa, Florida 33620, United States*

Christopher Stevens − *Department of Physics, University of South Florida, Tampa, Florida 33620, United States*

Hengzhou Liu − *Department of Physics, University of South Florida, Tampa, Florida 33620, United States*

Florence A. Nugera − *Department of Physics, University of South Florida, Tampa, Florida 33620, United States*

Nalaka Kapuruge − *Department of Physics, University of South Florida, Tampa, Florida 33620, United States*

Humberto Rodriguez Gutierrez − *Department of Physics, University of South Florida, Tampa, Florida 33620, United States;* orcid.org/0000-0001-8997-5274

Fang Liu − *Department of Chemistry, Stanford University, Stanford, California 94305, United States*

Xiaoyang Zhu − *Department of Chemistry, Columbia University, New York, New York 10027-6902, United States*

Dmitry Semenov − *National High Magnetic Field Laboratory, Florida State University, Tallahassee, Florida 30201, United States*

Stephen A. McGill − *National High Magnetic Field Laboratory, Florida State University, Tallahassee, Florida 30201, United States*

Nihar Pradhan − *Layered Materials and Device Physics Laboratory, Department of Chemistry, Physics and Atmospheric Science, Jackson State University, Jackson, Mississippi 39217, United States;* orcid.org/0000-0002-3912-4233

David J. Hilton − *Department of Physics, University of Alabama at Birmingham, Birmingham, Alabama 35294, United States;* orcid.org/0000-0003-2058-9062

Complete contact information is available at: https://pubs.acs.org/10.1021/acs.nanolett.1c04667

Author Contributions

Conceptualization: D.K., T.T., V.T., S.A.M. Methodology: D.K., T.T., V.T., S.A.M., F.L., X.Z., N.P. Investigation: V.M., A.B., T.T., C.S., H.L., F.A.N., N.K., D.S. Visualization: D.K., V.M., T.T. Supervision: D.K., H.R.G., X.Z., S.A.M., N.P., D.J.H. Writing (original draft): T.T., V.M., D.K. Writing (review and editing): D.K.

Notes

The authors declare no competing financial interest.

ACKNOWLEDGMENTS

The work was in part supported by the U.S. Department of Energy, Office of Basic Energy Sciences, Division of Materials Sciences and Engineering under Award No. DE-SC0012635. A portion of this work was performed at the National High Magnetic Field Laboratory, which is supported by the National Science Foundation Cooperative Agreement No. DMR-1644779 and the State of Florida. X.Y.Z. acknowledges support for sample preparation by the Materials Science and Engineering Research Center (MRSEC) through NSF Grant DMR-2011738. V.T. was in part was supported by the United

States Department of Energy under Grant No. DE-FG02-07ER46354.

REFERENCES

(1) Xiao, D.; Liu, G.-B.; Feng, W.; Xu, X.; Yao, W. Coupled Spin and Valley Physics in Monolayers of MoS_2 and Other Group-VI Dichalcogenides. *Phys. Rev. Lett.* **2012**, *108*, 196802.

(2) Mak, K.; McGill, K.; Park, J.; McEuen, P. The valley hall effect in MoS_2 transistors. *Science* **2014**, *344*, 1489−1492.

(3) MacNeill, D.; Heikes, C.; Mak, K. F.; Anderson, Z.; Kormányos, A.; Zólyomi, V.; Park, J.; Ralph, D. C. Breaking of Valley Degeneracy by Magnetic Field in Monolayer $MoSe_2$. *Phys. Rev. Lett.* **2015**, *114*, 037401.

(4) Roch, J. G.; Froehlicher, G.; Leisgang, N.; Makk, P.; Watanabe, K.; Taniguchi, T.; Warburton, R. J. Spin-polarized electrons in monolayer MoS_2. *Nat. Nanotechnol.* **2019**, *14*, 432−436.

(5) Chen, X.; Yan, T.; Zhu, B.; Yang, S.; Cui, X. Optical Control of Spin Polarization in Monolayer Transition Metal Dichalcogenides. *ACS Nano* **2017**, *11*, 1581−1587.

(6) Bawden, L.; Cooil, S. P.; Mazzola, F.; Riley, J. M.; Collins-McIntyre, L. J.; Sunko, V.; Hunvik, K. W. B.; Leandersson, M.; Polley, C. M.; Balasubramanian, T.; Kim, T. K.; Hoesch, M.; Wells, J. W.; Balakrishnan, G.; Bahramy, M. S.; King, P. D. C. Spin−valley locking in the normal state of a transition-metal dichalcogenide superconductor. *Nat. Commun.* **2016**, *7*, 11711.

(7) Xie, L.; Cui, X. Manipulating spin-polarized photocurrents in 2D transition metal dichalcogenides. *Proc. Natl. Acad. Sci. U. S. A.* **2016**, *113*, 3746−3750.

(8) Zhou, B. T.; Taguchi, K.; Kawaguchi, Y.; Tanaka, Y.; Law, K. T. Spin-orbit coupling induced valley Hall effects in transition-metal dichalcogenides. *Communications Physics* **2019**, *2*, 26.

(9) Mak, K. F.; He, K.; Shan, J.; Heinz, T. F. Control of valley polarization in monolayer MoS2 by optical helicity. *Nat. Nanotechnol.* **2012**, *7*, 494−498.

(10) Zeng, H.; Dai, J.; Yao, W.; Xiao, D.; Cui, X. Valley polarization in MoS2 monolayers by optical pumping. *Nat. Nanotechnol.* **2012**, *7*, 490−493.

(11) Srivastava, A.; Sidler, M.; Allain, A. V.; Lembke, D. S.; Kis, A.; Imamoğlu, A. Valley Zeeman effect in elementary optical excitations of monolayer WSe2. *Nat. Phys.* **2015**, *11*, 141−147.

(12) Cao, T.; Wang, G.; Han, W.; Ye, H.; Zhu, C.; Shi, J.; Niu, Q.; Tan, P.; Wang, E.; Liu, B.; Feng, J. Valley-selective circular dichroism of monolayer molybdenum disulphide. *Nat. Commun.* **2012**, *3*, 887.

(13) Kośmider, K.; González, J. W.; Fernández-Rossier, J. Large spin splitting in the conduction band of transition metal dichalcogenide monolayers. *Phys. Rev. B* **2013**, *88*, 245436.

(14) Zhang, X.-X.; Cao, T.; Lu, Z.; Lin, Y.-C.; Zhang, F.; Wang, Y.; Li, Z.; Hone, J. C.; Robinson, J. A.; Smirnov, D.; Louie, S. G.; Heinz, T. F. Magnetic brightening and control of dark excitons in monolayer WSe2. *Nat. Nanotechnol.* **2017**, *12*, 883−888.

(15) Deilmann, T.; Thygesen, K. S. Dark excitations in monolayer transition metal dichalcogenides. *Phys. Rev. B* **2017**, *96*, 201113.

(16) Feierabend, M.; Brem, S.; Ekman, A.; Malic, E. Brightening of spin- and momentum-dark excitons in transition metal dichalcogenides. *2D Materials* **2021**, *8*, 015013.

(17) Robert, C.; Han, B.; Kapuscinski, P.; Delhomme, A.; Faugeras, C.; Amand, T.; Molas, M. R.; Bartos, M.; Watanabe, K.; Taniguchi, T.; Urbaszek, B.; Potemski, M.; Marie, X. Measurement of the spin-forbidden dark excitons in MoS2 and MoSe2 monolayers. *Nat. Commun.* **2020**, *11*, 4037.

(18) Zhang, X.-X.; You, Y.; Zhao, S. Y. F.; Heinz, T. F. Experimental Evidence for Dark Excitons in Monolayer WSe_2. *Phys. Rev. Lett.* **2015**, *115*, 257403.

(19) Danovich, M.; Zólyomi, V.; Fal'ko, V. I.; Aleiner, I. L. Auger recombination of dark excitons in WS_2 and WSe_2 monolayers. *2D Materials* **2016**, *3*, 035011.

(20) Poellmann, C.; Steinleitner, P.; Leierseder, U.; Nagler, P.; Plechinger, G.; Porer, M.; Bratschitsch, R.; Schuller, C.; Korn, T.; Huber, R. Resonant internal quantum transitions and femtosecond radiative decay of excitons in monolayer WSe_2. *Nat. Mater.* **2015**, *14*, 889.

(21) Molas, M. R.; Faugeras, C.; Slobodeniuk, A. O.; Nogajewski, K.; Bartos, M.; Basko, D. M.; Potemski, M. Brightening of dark excitons in monolayers of semiconducting transition metal dichalcogenides. *2D Materials* **2017**, *4*, 021003.

(22) Vasconcelos, R.; Bragança, H.; Qu, F.; Fu, J. Dark exciton brightening and its engaged valley dynamics in monolayer WSe_2. *Phys. Rev. B* **2018**, *98*, 195302.

(23) Zhou, Y.; Scuri, G.; Wild, D. S.; High, A. A.; Dibos, A.; Jauregui, L. A.; Shu, C.; De Greve, K.; Pistunova, K.; Joe, A. Y.; Taniguchi, T.; Watanabe, K.; Kim, P.; Lukin, M. D.; Park, H. Probing dark excitons in atomically thin semiconductors via near-field coupling to surface plasmon polaritons. *Nat. Nanotechnol.* **2017**, *12*, 856−860.

(24) Park, K.-D.; Jiang, T.; Clark, G.; Xu, X.; Raschke, M. B. Radiative control of dark excitons at room temperature by nano-optical antenna-tip Purcell effect. *Nat. Nanotechnol.* **2018**, *13*, 59−64.

(25) Li, Z.; Wang, T.; Jin, C.; Lu, Z.; Lian, Z.; Meng, Y.; Blei, M.; Gao, S.; Taniguchi, T.; Watanabe, K.; Ren, T.; Tongay, S.; Yang, L.; Smirnov, D.; Cao, T.; Shi, S.-F. Emerging photoluminescence from the dark-exciton phonon replica in monolayer WSe2. *Nat. Commun.* **2019**, *10*, 2469.

(26) Stevens, C. E.; Paul, J.; Cox, T.; Sahoo, P. K.; Gutiérrez, H. R.; Turkowski, V.; Semenov, D.; McGill, S. A.; Kapetanakis, M. D.; Perakis, I. E.; Hilton, D. J.; Karaiskaj, D. Biexcitons in monolayer transition metal dichalcogenides tuned by magnetic fields. *Nat. Commun.* **2018**, *9*, 3720.

(27) Aivazian, G.; Gong, Z.; Jones, A. M.; Chu, R.-L.; Yan, J.; Mandrus, D. G.; Zhang, C.; Cobden, D.; Yao, W.; Xu, X. Magnetic control of valley pseudospin in monolayer WSe2. *Nat. Phys.* **2015**, *11*, 148−152.

(28) Zhao, C.; et al. Enhanced valley splitting in monolayer WSe2 due to magnetic exchange field. *Nat. Nanotechnol.* **2017**, *12*, 757−762.

(29) Xiao, D.; Liu, G.-B.; Feng, W.; Xu, X.; Yao, W. Coupled Spin and Valley Physics in Monolayers of MoS_2 and Other Group-VI Dichalcogenides. *Phys. Rev. Lett.* **2012**, *108*, 196802.

(30) Dey, P.; Paul, J.; Wang, Z.; Stevens, C. E.; Liu, C.; Romero, A. H.; Shan, J.; Hilton, D. J.; Karaiskaj, D. Optical Coherence in Atomic-Monolayer Transition-Metal Dichalcogenides Limited by Electron-Phonon Interactions. *Phys. Rev. Lett.* **2016**, *116*, 127402.

(31) Jakubczyk, T.; Delmonte, V.; Koperski, M.; Nogajewski, K.; Faugeras, C.; Langbein, W.; Potemski, M.; Kasprzak, J. Radiatively Limited Dephasing and Exciton Dynamics in $MoSe_2$ Monolayers Revealed with Four-Wave Mixing Microscopy. *Nano Lett.* **2016**, *16*, 5333−5339.

(32) Moody, G.; Kavir Dass, C.; Hao, K.; Chen, C.-H.; Li, L.-J.; Singh, A.; Tran, K.; Clark, G.; Xu, X.; Berghäuser, G.; Malic, E.; Knorr, A.; Li, X. Intrinsic homogeneous linewidth and broadening mechanisms of excitons in monolayer transition metal dichalcogenides. *Nat. Commun.* **2015**, *6*, 8315.

(33) Martin, E. W.; Horng, J.; Ruth, H. G.; Paik, E.; Wentzel, M.-H.; Deng, H.; Cundiff, S. T. Encapsulation Narrows and Preserves the Excitonic Homogeneous Linewidth of Exfoliated Monolayer $MoSe_2$. *Phys. Rev. Applied* **2020**, *14*, 021002.

(34) Palummo, M.; Bernardi, M.; Grossman, J. C. Exciton Radiative Lifetimes in Two-Dimensional Transition Metal Dichalcogenides. *Nano Lett.* **2015**, *15*, 2794−2800.

(35) Deveaud, B.; Clérot, F.; Roy, N.; Satzke, K.; Sermage, B.; Katzer, D. S. Enhanced radiative recombination of free excitons in GaAs quantum wells. *Phys. Rev. Lett.* **1991**, *67*, 2355−2358.

(36) Leo, K.; Göbel, E. O.; Damen, T. C.; Shah, J.; Schmitt-Rink, S.; Schäfer, W.; Müller, J. F.; Köhler, K.; Ganser, P. Subpicosecond four-wave mixing in $GaAs/Al_xGa_{1-x}As$ quantum wells. *Phys. Rev. B* **1991**, *44*, 5726−5737.

(37) Smirl, A. L.; Stevens, M. J.; Chen, X.; Buccafusca, O. Heavy-hole and light-hole oscillations in the coherent emission from quantum wells: Evidence for exciton-exciton correlations. *Phys. Rev. B* **1999**, *60*, 8267−8275.

https://doi.org/10.1021/acs.nanolett.1c04667
Nano Lett. 2022, 22, 1680−1687

(38) Phillips, M.; Wang, H. Coherent oscillation in four-wave mixing of interacting excitons. *Solid State Commun.* **1999**, *111*, 317−321.
(39) Weber, D.; Petri, W.; Woggon, U.; Klingshirn, C. F.; Shevel, S.; Göbel, E. O. Quantum beats of exciton polaritons in hexagonal CdS crystals. *Phys. Rev. B* **1997**, *55*, 12848−12851.
(40) Shepard, G. D.; Ardelean, J. V.; Ajayi, O. A.; Rhodes, D. A.; Zhu, X.; Hone, J. C.; Strauf, S. Trion-Species-Resolved Quantum Beats in $MoSe_2$. *ACS Nano* **2017**, *11*, 11550−11558.
(41) Sim, S.; Lee, D.; Trifonov, A. V.; Kim, T.; Cha, S.; Sung, J. H.; Cho, S.; Shim, W.; Jo, M.-H.; Choi, H. Ultrafast quantum beats of anisotropic excitons in atomically thin ReS2. *Nat. Commun.* **2018**, *9*, 351.
(42) Von Plessen, G.; Koch, M.; Feldmann, J.; Göbel, E.; Thomas, P.; Shah, J.; Köhler, K. *Coherent Optical Interactions in Semiconductors*; Springer, 1994; pp 289−293.
(43) Kojima, O.; Mizoguchi, K.; Nakayama, M. Coupling of coherent longitudinal optical phonons to excitonic quantum beats in GaAs/AlAs multiple quantum wells. *Phys. Rev. B* **2003**, *68*, 155325.
(44) Hao, K.; Specht, J. F.; Nagler, P.; Xu, L.; Tran, K.; Singh, A.; Dass, C. K.; Schüller, C.; Korn, T.; Richter, M.; Knorr, A.; Li, X.; Moody, G. Neutral and charged inter-valley biexcitons in monolayer MoSe2. *Nat. Commun.* **2017**, *8*, 15552.
(45) Hao, K.; Xu, L.; Nagler, P.; Singh, A.; Tran, K.; Dass, C. K.; Schüller, C.; Korn, T.; Li, X.; Moody, G. Coherent and Incoherent Coupling Dynamics between Neutral and Charged Excitons in Monolayer MoSe2. *Nano Lett.* **2016**, *16*, 5109−5113.
(46) Li, Y.; Ludwig, J.; Low, T.; Chernikov, A.; Cui, X.; Arefe, G.; Kim, Y. D.; van der Zande, A. M.; Rigosi, A.; Hill, H. M.; Kim, S. H.; Hone, J.; Li, Z.; Smirnov, D.; Heinz, T. F. Valley Splitting and Polarization by the Zeeman Effect in Monolayer $MoSe_2$. *Phys. Rev. Lett.* **2014**, *113*, 266804.
(47) Stier, A. V.; Wilson, N. P.; Velizhanin, K. A.; Kono, J.; Xu, X.; Crooker, S. A. Magnetooptics of Exciton Rydberg States in a Monolayer Semiconductor. *Phys. Rev. Lett.* **2018**, *120*, 057405.
(48) Chemla, D.; Shah, J. Many-body and correlation effects in semiconductors. *Nature* **2001**, *411*, 549−557.
(49) Lozovik, Y. E.; Ovchinnikov, I. V.; Volkov, S. Y.; Butov, L. V.; Chemla, D. S. Quasi-two-dimensional excitons in finite magnetic fields. *Phys. Rev. B* **2002**, *65*, 235304.

https://doi.org/10.1021/acs.nanolett.1c04667
Nano Lett. 2022, 22, 1680−1687